Electronic Supplementary Material (ESI) for Chemical Communications.

Supplementary information

Nanoceria Decorated Flower-like Molybdenum Sulphide Nanoflakes: An Efficient Nanozyme to Tumour Selective ROS Generation and Photo Thermal Therapy

Chandran Murugan,[a] Nagaraj Murugan,[b] Ashok K. Sundramoorthy,[b] Anandhakumar Sundaramurthy [a,c]*

[a]SRM Research Institute, SRM Institute of Science and Technology, Kattankulathur 603203, Kanchipuram, India.

[b]Department of Chemistry, SRM Institute of Science and Technology, Kattankulathur 603203, Kanchipuram, India.

[c]Department of Physics and Nanotechnology, SRM Institute of Science and Technology, Kattankulathur 603203, Kanchipuram, India.

Materials and Methods

Sodium molybdate dehydrate ($Na_2MoO_4 \cdot 2H_2O$), thiourea (CH_4N_2S), L-Cysteine, branched polyethylenimine (Mw~25,000), ethylene glycol, cerium (III) nitrate hexahydrate ($Ce(NO_3)_3.6H_2O$), sodium hydroxide (NaOH), hydrochloric acid (HCl). All reagents used in this work were of analytical grade and used as received without any further purification.

Synthesis of flower-like Molybdenum disulphide (MoS_2) nanoflakes

Flower-like MoS_2 nanoflakes were synthesized by hydrothermal method at 200 ˚C for 24 h. In brief, the starting solution was prepared by mixing 50 mg of $Na_2MoO_4.2H_20$ and 35 mg of thiourea in 50 mL of milliQ water. The mixture was sonicated for 10 min at room temperature (RT), and subsequently adjusted to pH 3 by adding 0.1 M HCl. The mixture was then transferred to a teflon-lined stainless-steel autoclave and heated to 200 ˚C for 24 h in a hot air oven (220 V, 50Hz, Jothi enterprises Pvt. Ltd., India). After completion of the reaction, the black color precipitate obtained was separated by centrifugation at 8000 rpm for 15 min and washed several times with milliQ water and ethanol to remove the impurities. The MoS_2 powder was obtained by drying the precipitate under vacuum at 80 ˚C overnight.

Synthesis of PEI coated flower-like MoS_2 nanoflakes (MoS_2-PEI)

In a round bottom flask, 0.2 g of MoS_2 nanoflakes and 25 mg of L-cysteine was dispersed in 25 mL of milliQ water at 37 ˚C under continuous stirring. After 4 h of stirring at room temperature, subsequently drop wise added 0.50 g and 0.30 g of EDC/NHS and adjust the reaction mixture pH6.8. Stirring for few hours, afterwards, 1% PEI solution prepared in ethanol was added in a drop-wise manner to form PEI coated MoS_2 nanoflakes. Stirring process was continued for another 4 h. After reaction, the final product was separated by centrifugation and washed with milliQ water and ethanol for several times. The resultant nanostructures (PEI-MoS_2) were dried overnight under vacuum.

Synthesis of Nanoceria by ethylene glycol-assisted precipitation method

The nanoceria (($NCeO_2$) was prepared by Ethylene glycol-assisted precipitation method, For this, 25 mg of $Ce(NO_3)_2.6H_20$, 0.250 µL of Ethylene glycol (95%) and 200 µL of 0.5 M NaOH was dissolved in 50 mL of Milli-Q water and the solution was kept overnight under mild stirring. The product obtained was collected by centrifugation and washed several times with milliQ water and ethanol. The final product was dried at 180 ˚C for 6 h using muffle furnace (3 kW, Jothi enterprises Pvt. Ltd., India). After cooling the sample to room temperature, the powder was washed with water for 10 min under ultra-sonication and dried under vacuum.

Synthesis of $NCeO_2$ decorated PEI coated flower-like MoS_2 ($NCeO_2$-PEI-MoS_2) nanoflake

Briefly, the different concentration (0.25, 0.50, 0.75 and 1.0 mg/mL) of as-synthesized $NCeO_2$ and 100 mg of PEI -MoS_2 nanoflakes was added in 50 mL of milli-Q water and the mixture was stirred overnight at room temperature. Flakes were collected and purified by repeated centrifugation and washing steps with water and ethanol. The final product ($NCeO_2$ decorated flower-like MoS_2 nanoflakes) was dried under vacuum and stored for further use.

Nanomaterial characterization

The morphological features and composition of as-synthesized nanomaterials were investigated using transmission electron microscopy (TEM) and the elemental distribution was analyzed via energy dispersive X-ray spectroscopy (TEM-EDX, JEOL JEM-2100). For TEM-EDX analysis, 4 µL of diluted suspensions of bare MoS_2 nanoflakes, $NCeO_2$-PEI-MoS_2 nanoflakes and $NCeO_2$ were placed on carbon-coated copper grids and dried overnight at room temperature to remove the moisture completely. TEM images of all the samples were acquired using a HR-TEM at an accelerating voltage of 200 kV. For X-ray diffraction (XRD) investigations, the powder samples of MoS_2 nanoflakes (bare and decorated) and $NCeO_2$ were used for analysis in a D/max-2550 PC X-ray diffractometer (XRD; Rigaku, Japan) from 10 to 90˚. Raman spectrum was acquired in Via-Reflex micro-raman spectroscopy system (Renishaw, UK) with a laser

wavelength of 532 nm. The powder samples of MoS_2, MoS_2-PEI, $NCeO_2$, and $NCeO_2$-PEI-MoS_2 nanoflakes were mixed with KBr powder and made into pellets. The spectrum was acquired in transmission mode with the scanning range of 4000-400 cm^{-1} using Fourier transform infra-red (FTIR, Nicolet 6700 (Thermo Fisher, USA)) spectrometer.

Cell line and cell culture condition

Normal breast cell line (HB-100) and experimental breast cancer cell line MDA-MB-231 cells were obtained from National Centre for Cell Sciences (NCCS), Pune, India. Then, the cell line was maintained in Dulbecco's Modified Eagle Medium (DMEM) media with addition of proper supplements such as 10% (v/v) FBS, 1% (v/v), 100 µg/mL streptomycin and 100 U/mL penicillin. Then, the cells were grown in a humidified incubator at 37 °C under atmosphere supplemented with 95% air and 5% CO_2. The cell culture medium was changed every day, and cells were always trypsinized and harvested before reaching confluence so that they were never subject to crowded conditions.

Cell viability assay

Normal breast cell line (HB-100) and experimental breast cancer cell line MDA-MB-231 cells were plated in 96-well plates at a density of 1×10^5 cells/well and grown for 24 h. The cells were then treated with various concentrations (6, 12, 25, 50, 100, 150 and 200 µg/mL) of bare flower-like MoS_2 nanoflakes, $NCeO_2$-PEI-MoS_2 (0.25 mg/mL), $NCeO_2$-PEI-MoS_2 (0.50 mg/mL), $NCeO_2$-PEI-MoS_2 (0.75 mg/mL), and $NCeO_2$-PEI-MoS_2 (1.0 mg/mL) nanoflakes at 37 °C for 24 h. After washing the cells with PBS to remove unbound nanoflakes, 20 µL MTT solution (3-(4, 5-dimethylthiazol-2-yl)-3 2, 5-diphenyltetrazolium bromide) at 0.5 mg mL^{-1} were dropped into the 96-well plate for MTT assay. The cell viability was calculated as a percentage of viable cells after treated with nanomaterials when compared to the untreated cells. It is worth noting that $NCeO_2$-PEI-MoS_2 nanoflakes displayed excellent physiological stability in water, PBS and cell culture medium even after 24 h storage.

Measurement of Intracellular ROS generation

To obtain quantitative information about the intracellular free radicals such as peroxide and superoxide free radicals, 5 μg/mL of 2', 7'-Dichlorofluorescein diacetate (DCFH-DA) was added to each well in a 6-well plate containing 5×10^5 cells/well. Samples with final concentration of 200 μg/mL of bare MoS_2, $NCeO_2$-PEI-MoS_2 (0.25 mg/mL), $NCeO_2$-PEI-MoS_2 (0.50 mg/mL), $NCeO_2$-PEI-MoS_2 (0.75 mg/mL), and $NCeO_2$-PEI-MoS_2 (1.0 mg/mL) were added to each well and incubated at 37 °C for 24 h in an incubator. The fluorescence intensity of DCF is proportional to the amount of ROS produced by the cell. ROS generation was assessed using a fluorescence microscope (Nikon Eclipse, Inc., Japan) and fluorescence intensity was assessed by fluorescent plate reader at excitation and emission wavelengths of 488 and 530 nm, respectively.

For synergistic effects of ROS and PTT assessment, same procedure mentioned above was performed with laser light irradiation at 808 nm for 5 min. After irradiation, the cells were incubated for 24 h, rinsed with PBS, and stained with 20 μM DCFH-DA for 20 min. Subsequently, the fluorescence intensity of DCF in each well was quantitatively estimated by a fluorescence microplate reader.

NIR laser-induced heat conversion of bare MoS_2 and $NCeO_2$-PEI-MoS_2 nanoflakes

Photothermal Performance experiments of bare MoS_2, and different concentrations (0.25, 0.50, 0.75 and 1.0 μg/mL) of $NCeO_2$ decorated PEI coated MoS_2 nanoflakes were carried out to examine the photothermal conversion effect by a laser light source at 808 nm (continuous-wave NIR laser device with power of 0.5 W/cm^2). 0.4 mL of aqueous suspensions containing 100 μg/mL of bare MoS_2 nanoflakes or $NCeO_2$ decorated MoS_2 nanoflakes were placed in a cuvette and irradiated with 808-nm NIR laser at a power of 0.5 W/cm^2. The temperature increase was monitored for every 20 s using a thermocouple

thermometer to determine the PCE of bare MoS_2 and $NCeO_2$-PEI-MoS_2 nanoflakes. Control experiments were performed with only water.

***In vitro* photothermal performance of bare MoS_2 and $NCeO_2$-PEI-MoS_2 nanoflakes**

Typically, MDA-MB-231 cells were incubated in 6-well plates at 37 °C with 5% CO_2 for 24 h. After replacing the medium with pre-warmed new culture medium, bare MoS_2 and different concentrations (0.25, 0.50, 0.75 and 1.0 mg/mL) of $NCeO_2$ decorated PEI coated MoS_2 nanoflakes (100 μg/mL) were added into the wells. After 5 h of incubation, cells were irradiated with 808-nm laser at a power density of 0.5 W/cm^2 for 5 min. The cells were then co-stained with florescent molecules acridine orange and propidium iodide and investigated in fluorescent microscope to visualize the live and dead cells. Finally, the viability of MDA-MB-231 cells was determined by fluorescent microscopy. The cell viability was normalized by control group without any treatment.

Statistical Analysis

The data obtained here are analyzed by student t-tests with a setting significance of $p < 0.05$ (*).

Results and Discussion

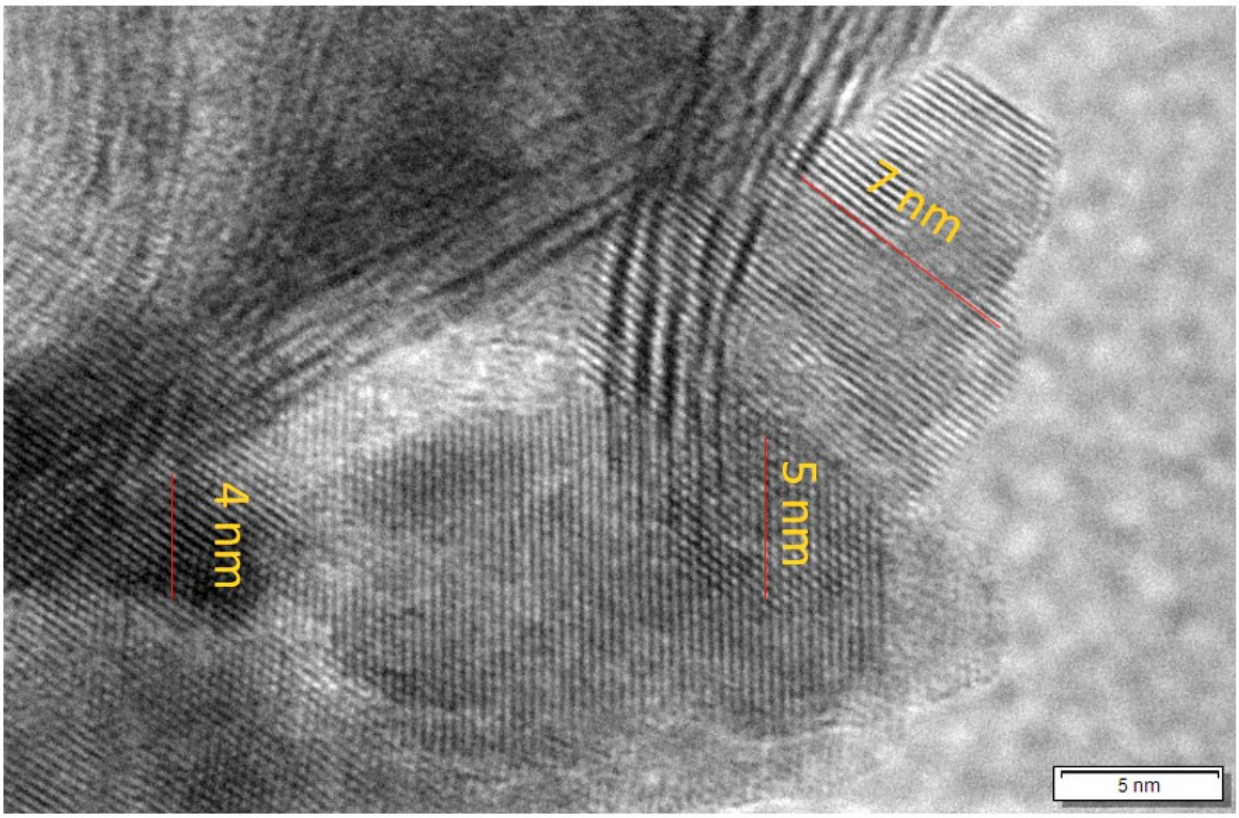

Figure S1. HR-TEM image reveals the size of spherical shaped $NCeO_2$ decoration onto PEI-MoS_2 nanoflakes.

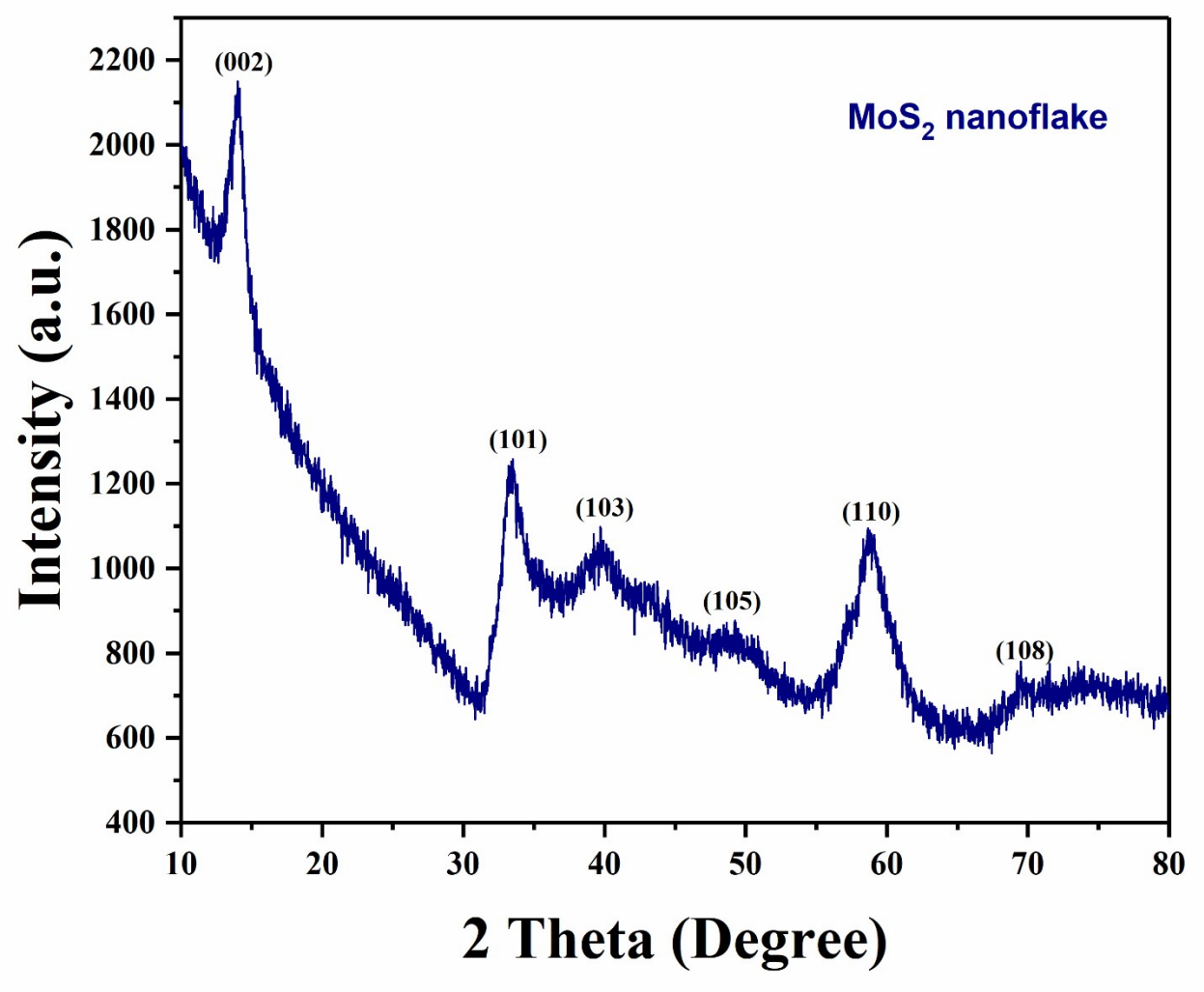

Figure S2. XRD pattern of flower-like MoS_2 nanoflake.

Fig. S2 shows the crystal structure of flower-like MoS_2 nanoflakes assessed by the powder X-ray diffraction (XRD) studies. The diffraction peaks observed at 14˚, 32˚, 39.5˚, and 58˚ are corresponding to (002), (100), (103), and (110) crystal planes of MoS_2 structure, consistent with the corresponding standard card (JCPDS card number 37-1492).

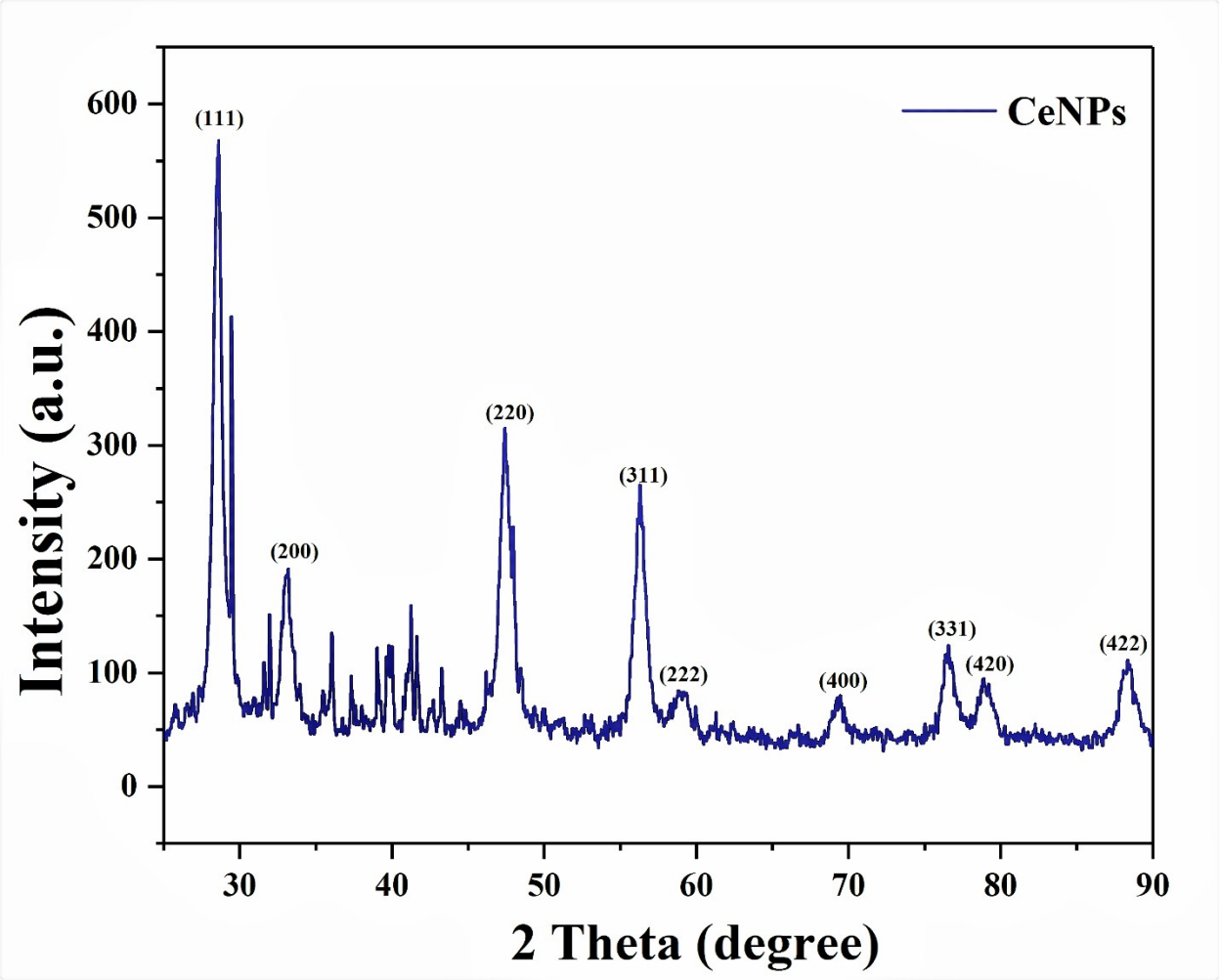

Figure S3. XRD pattern of crystalline structure of nanoceria.

Detailed study of structural identification of nanoceria was performed with X-ray diffraction (XRD) in the range of angle 2θ between 20˚ and 80 ˚, as shown in Fig.S3. The primary diffraction peaks are indexed as (111), (200), (220), (311), (222), (400), (331), and (422) reflections corresponding to $NCeO_2$, which clearly indicated the semi-crystalline and single phase of $NCeO_2$.

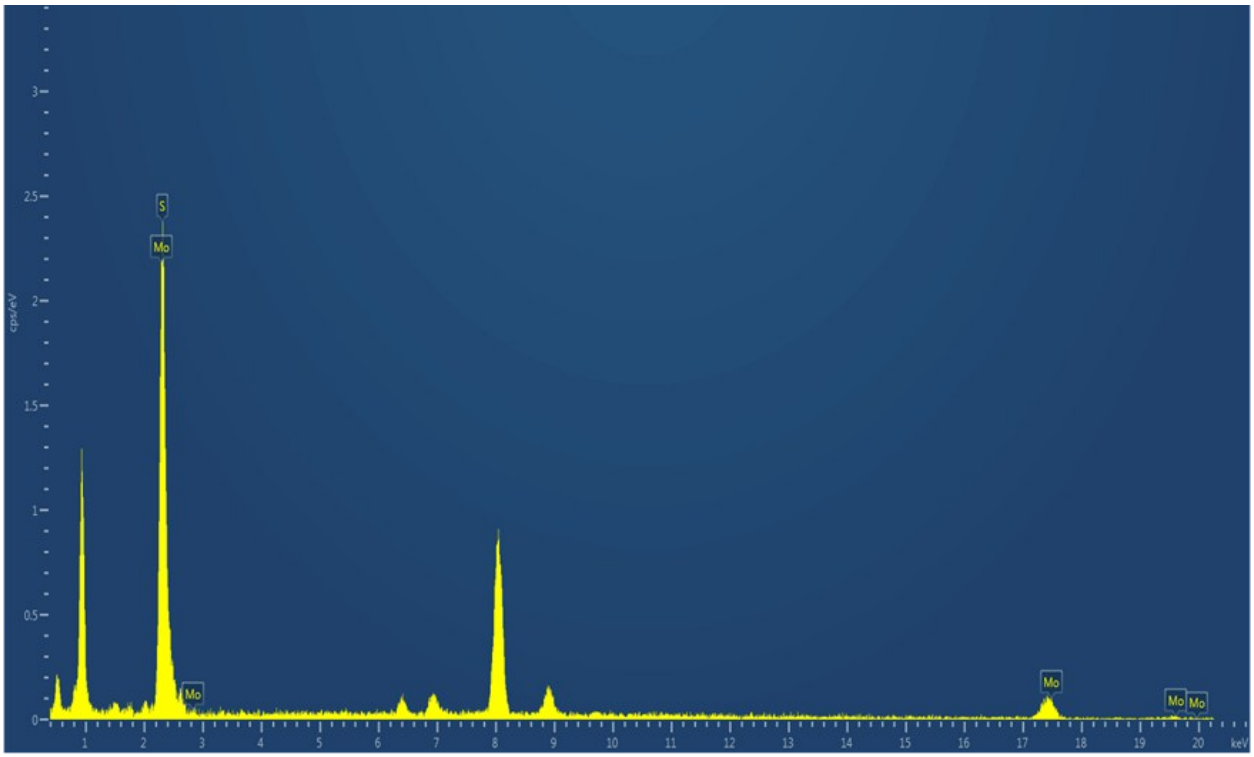

Figure S4. EDX pattern of flower-like MoS_2 nanoflakes. Note that carbon and copper peaks come from the carbon coated copper grids are not labeled.

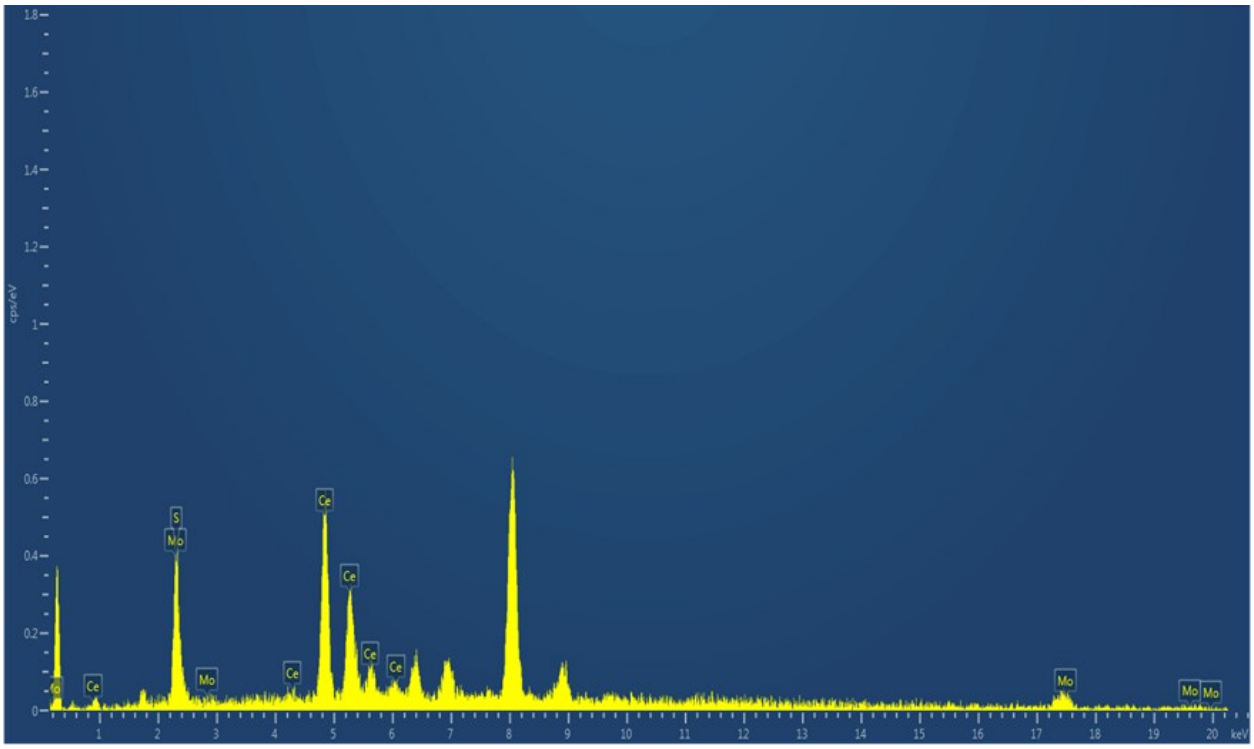

Figure S5. EDX pattern of $NCeO_2$ decorated PEI coated flower-like MoS_2 nanoflakes. Note that carbon and copper peaks come from the carbon coated copper grids are not labeled.

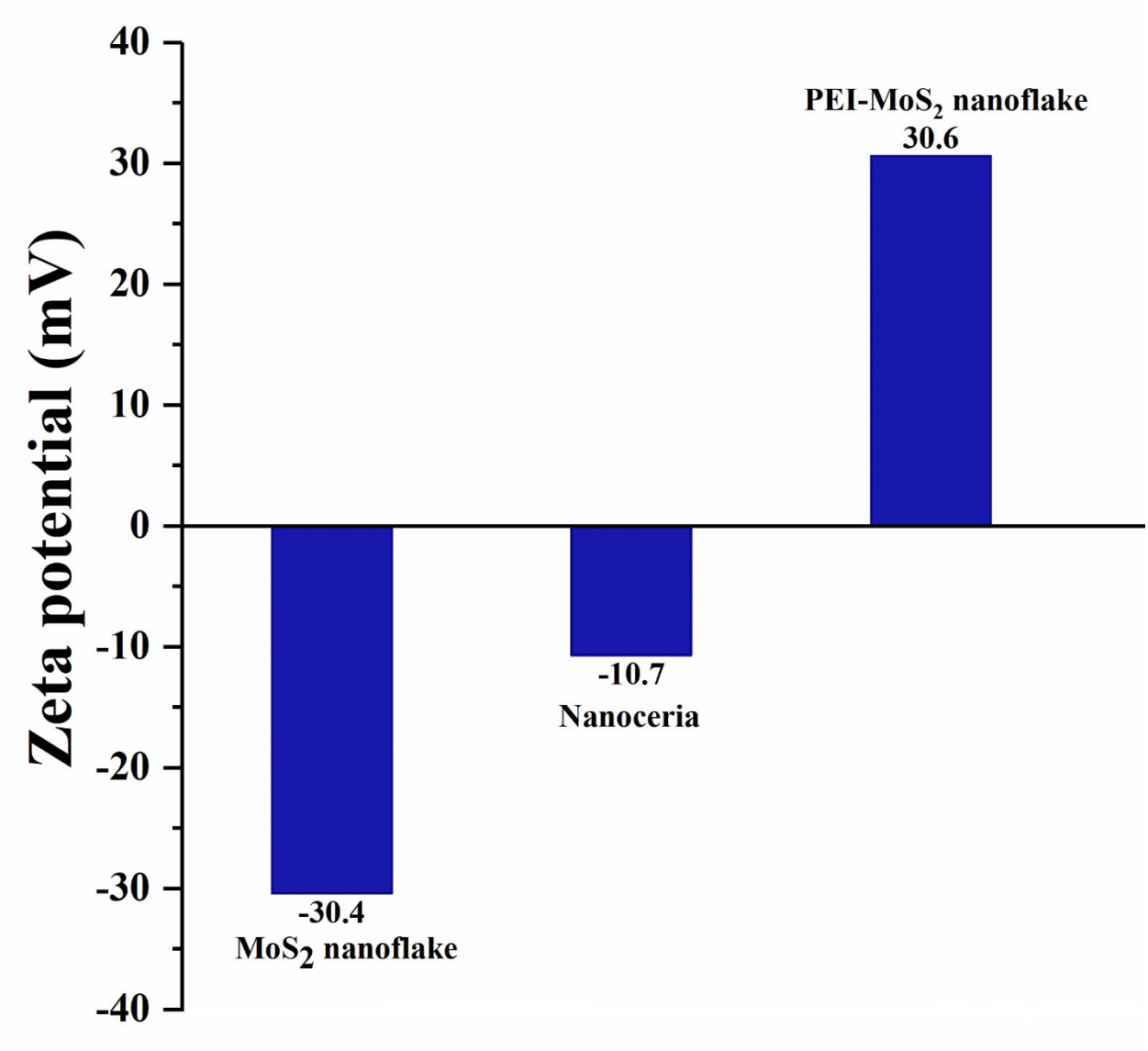

Figure S6. Zeta potential of flower-like MoS_2 nanoflakes, nanoceria and PEI coated MoS_2 nanoflakes.

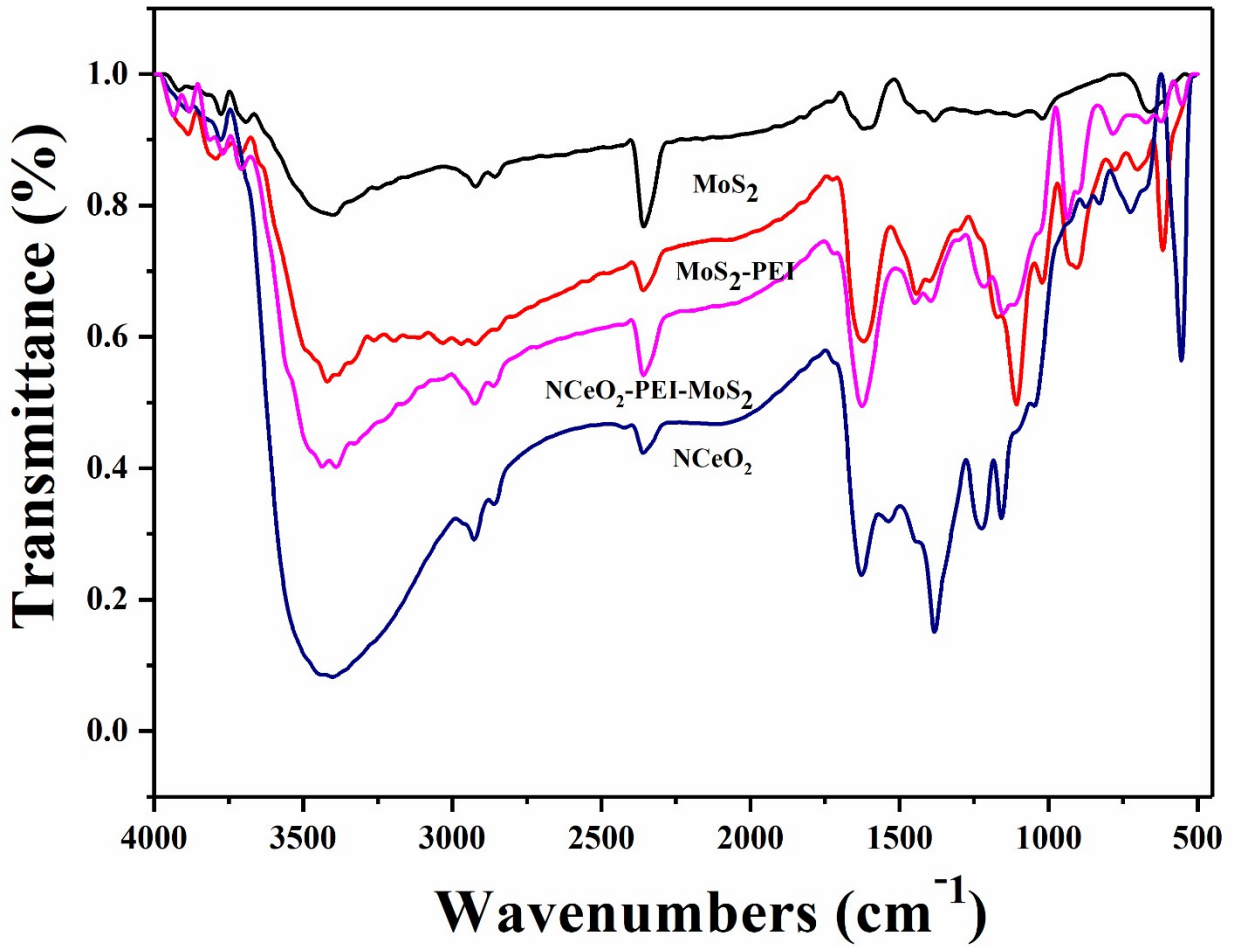

Figure S7. FTIR absorbance spectra of flower-like MoS_2, PEI coated flower-like MoS_2, $NCeO_2$, and $NCeO_2$-PEI-MoS_2 nanoflakes.

The surface functionalization of bare flower-like MoS_2, PEI coated flower-like MoS_2, nanoceria, and MoS_2-$NCeO_2$ were evaluated by FTIR spectroscopy (Figure S7). FTIR spectrum for bare flower-like MoS_2 nanoflakes showed a broad absorption band at 3416 cm^{-1}, indicating the stretching vibration of hydroxyl groups in the MoS_2 sample. The peaks observed at 1100, 1650 and 900 cm^{-1} are ascribed to the stretching vibrations of the hydroxyl groups, Mo-O vibrations, and formation of S-S bond. The FTIR spectrum of PEI coated flower-like MoS_2 showed peaks at 1393, 2847 and 1393 cm^{-1}, which are corresponding to NH_2-scissoring vibrations and vibrations of ethylene groups of PEI. The shifting of hydroxyl groups from 3416 to 3363 cm^{-1}, and formation of intense peaks at 1625 cm^{-1} indicates formation

of amide bond between cysteine residues on MoS_2 and PEI. It confirmed the successful deposition of PEI layer on the surface of the MoS_2 nanoflake. FTIR spectra of nanoceria clearly showed four intense peaks situated at 3423, 1625, 1380 and 542 cm^{-1}, which are corresponding to stretching vibration of hydroxyls groups, bending vibration of absorbed molecular water, O-C-O stretchings band and characteristic peak of $NCeO_2$ (Ce–O). FTIR spectrum of nanoceria decorated flower-like MoS_2 nanoflakes ($NCeO_2$-PEI-MoS_2) showed characteristic peaks of MoS_2 flakes, $NCeO_2$ and PEI, confirmed the successful conjugation of $NCeO_2$ on to the MoS2-PEI nanoflakes.

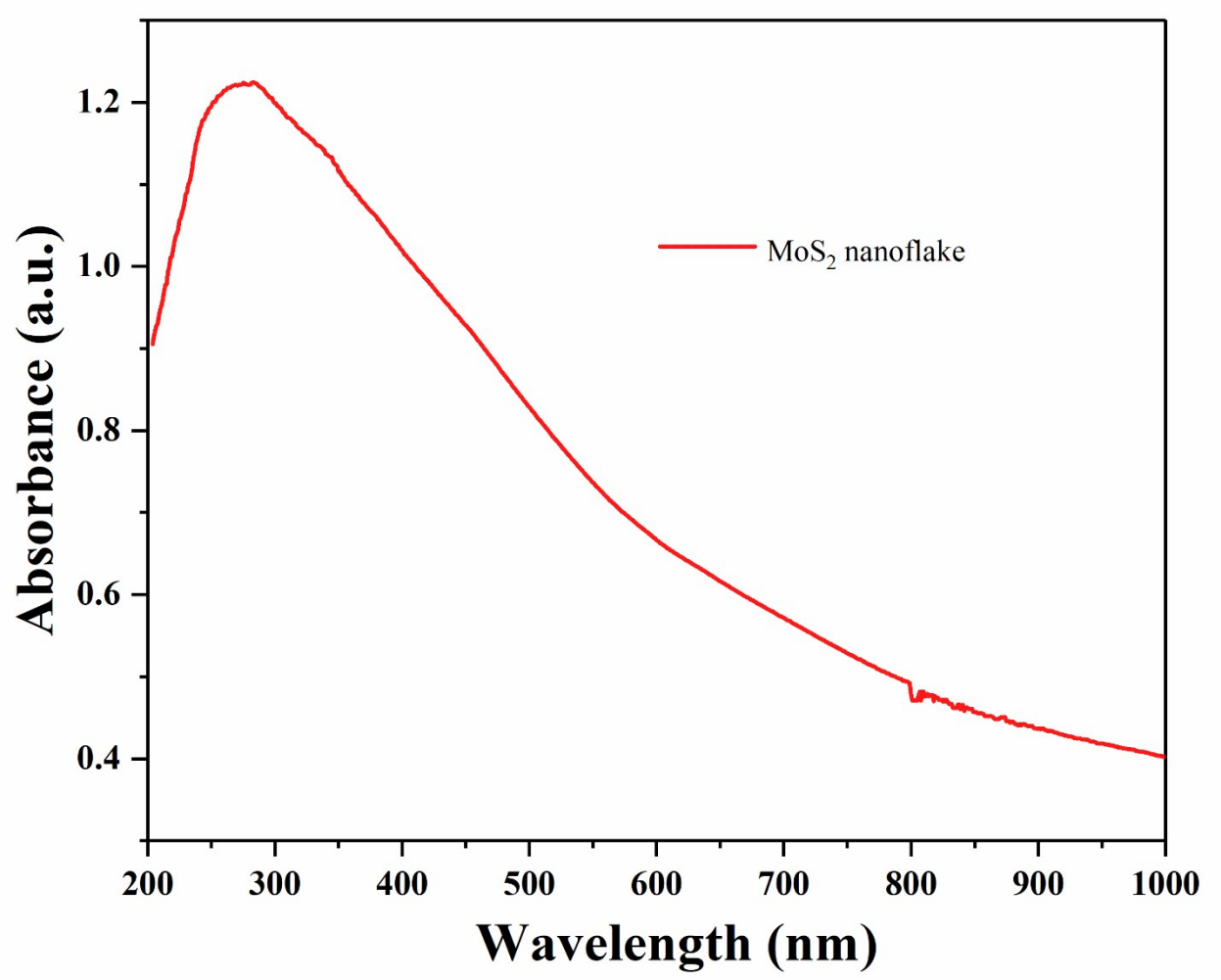

Figure S8. UV-Vis-NIR spectrum of flower-like MoS_2 nanoflakes.

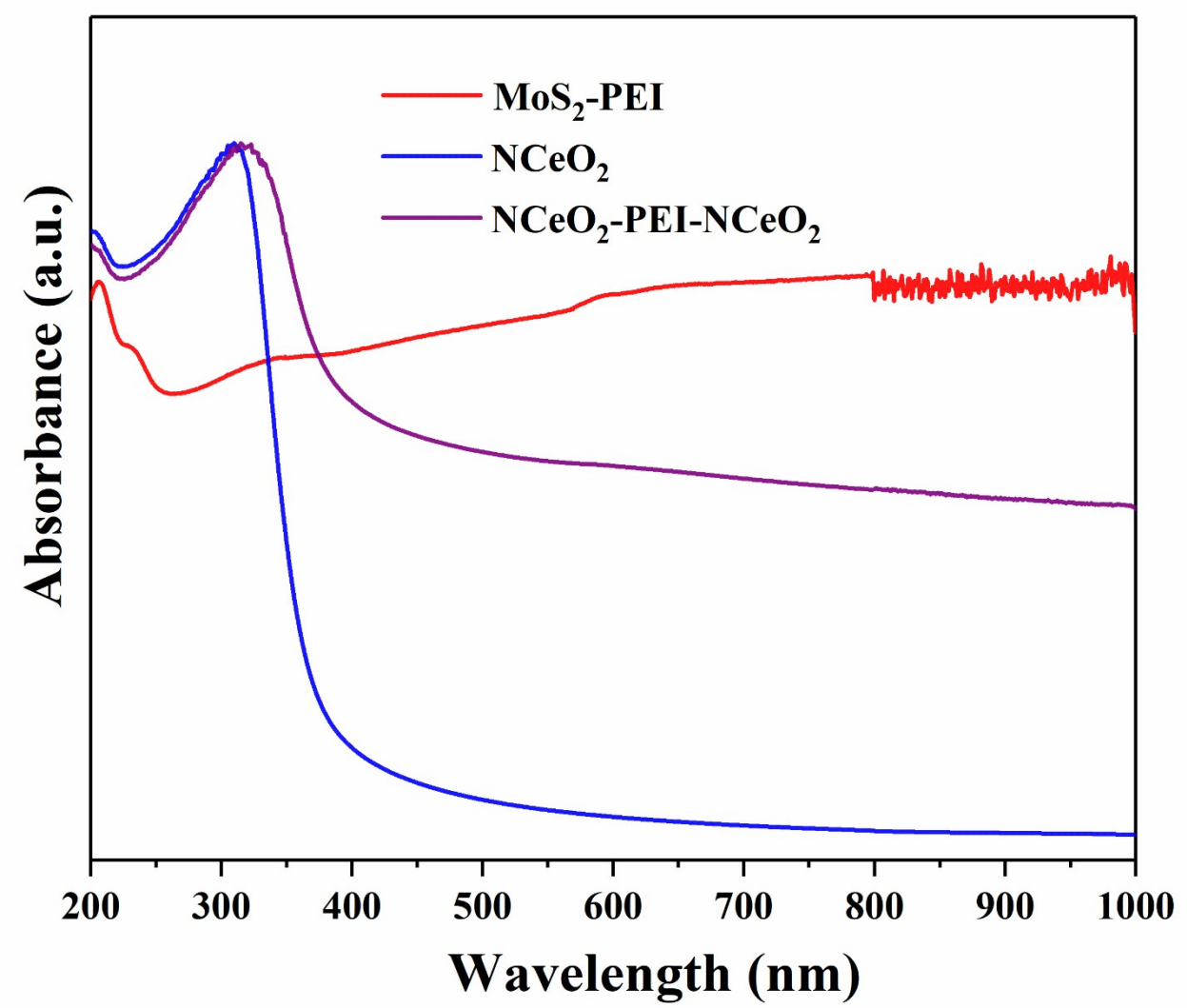

Figure S9. UV-Vis-NIR spectra of $NCeO_2$, PEI coated MoS_2 and flower-like MoS_2 nanoflakes.

UV-Vis absorption spectra of MoS_2, MoS_2-PEI, and $NCeO_2$-PEI-MoS_2 nanoflakes were acquired in transmission mode in aqueous dispersions. There are two absorption shoulder peaks in the visible region for PEI, and $NCeO_2$ has characteristic absorption peak at 308 nm. UV-Vis-NIR spectrum of $NCeO_2$-PEI-MoS_2 nanoflakes reveals a broader peak at 320 nm, indicating the decoration of $NCeO_2$ on to surface of MoS_2-PEI.

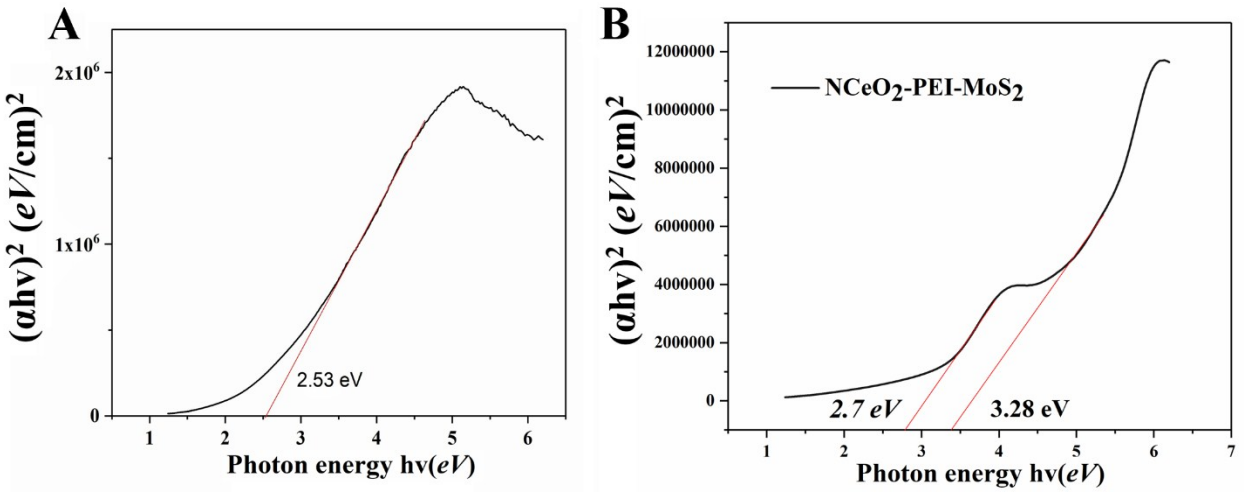

Figure S10. The bandgap energies of bare MoS_2 nanoflakes and $NCeO_2$-PEI-MoS_2 nanoflakes by Tauc plot method.

Based on the UV-Vis-NIR and Raman spectra of $NCeO_2$-PEI-MoS_2 nanoflakes, it was observed that intensities of $E1_{2g}$ and A_{1g} peaks were reduced and red shifted, demonstrating the decrease in crystallinities of the composites (1). Combining a wide-band-gap material ($NCeO_2$) with a smaller-band-gap semiconductor metal dichalcogenides (MoS_2) harvests a broader spectrum absorption of solar energy and promotes charge separation (2). The unique ability to tune the band gap to 2.7 eV and easier degradation of $NCeO_2$-PEI-MoS_2 nanoflakes made them as excellent photothermal agents for cancer PTT. For pure ceria, a single intense band centered at 459 cm^{-1} was observed, which signifies that there is apparently no extrinsic oxygen vacancy (3). When compared to the pure $NCeO_2$, the peak intensity was broader and blue-shifted to 446 cm^{-1} for $NCeO_2$-PEI-MoS_2 nanoflakes. Possible reason for shifting and broadening of the peak was the increase in number of oxygen vacancies, owing to the extrinsic oxygen vacancies introduced into the ceria when the Ce^{4+} ions are replaced by MoS_2 ions. The additional peak formed at 550-600 cm^{-1} is due to the structural defects derived from partial incorporation of $NCeO_2$ into MoS_2 lattice. When compared to bare MoS_2 nanoflakes, the Raman spectrum of $NCeO_2$-PEI-MoS_2 nanoflakes indicated $E1_{2g}$ mode shift as a function of biaxial strain in the bare MoS_2, and confirmed the $NCeO_2$ decoration on to MoS_2 nanoflakes. The disorder in MoS_2 nanoflakes has been related to the mechanical strain induced in the MoS_2 layer by the PEI coating and $NCeO_2$ decoration (4). The effective optical band gaps of the MoS_2 and $NCeO_2$-PEI-MoS_2 nanoflakes were 2.53 eV and 2.7 eV, respectively, indicating a 0.17 eV difference. This shows that the $NCeO_2$ acted as a band gap modifier.

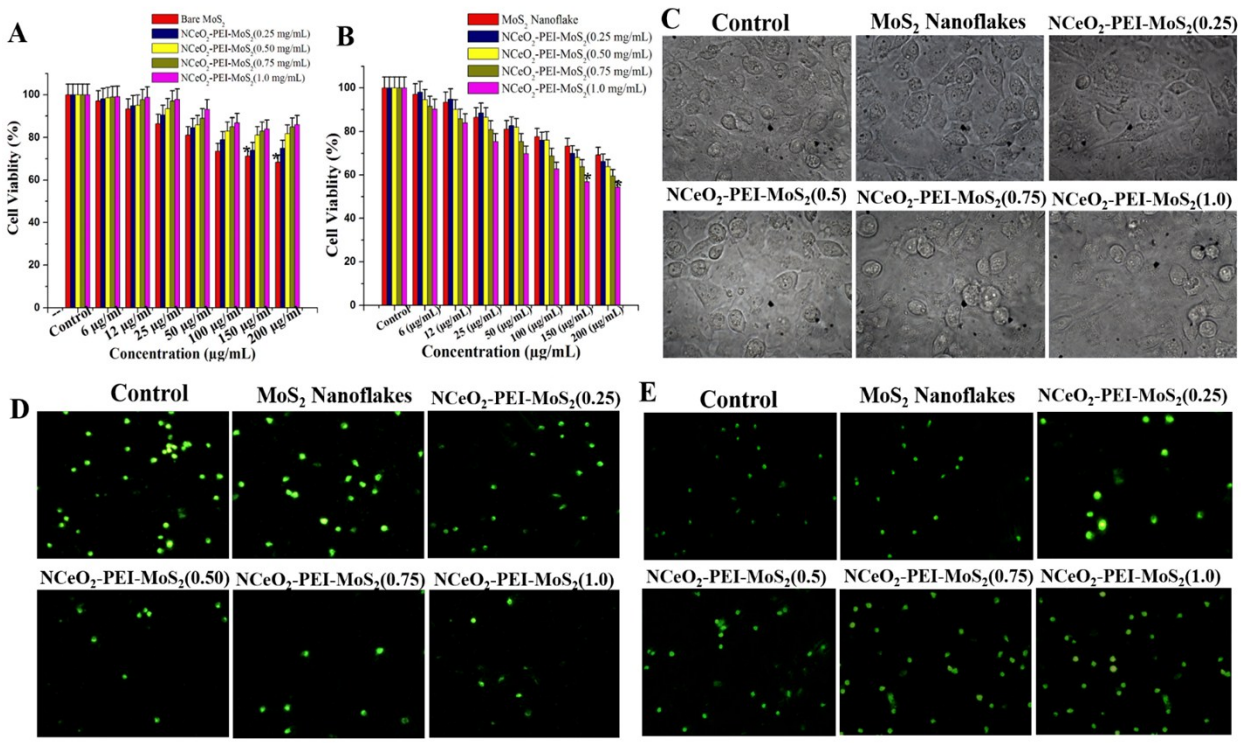

Figure S11. Evaluation of cell viability as a function of nanoflakes and $NCeO_2$ concentration by MTT assay. (A) HBL-100, (B and C) MDA-MB-231 cells treated with different nanoformulations at various concentrations (6-200 µg/mL) for 24 h at 37 °C . Fluorescence images of DCFH-DA stained (D) HBL-100 and (E) MDA-MB-231 cells showed the effect of different nanoformulations on ROS generation.

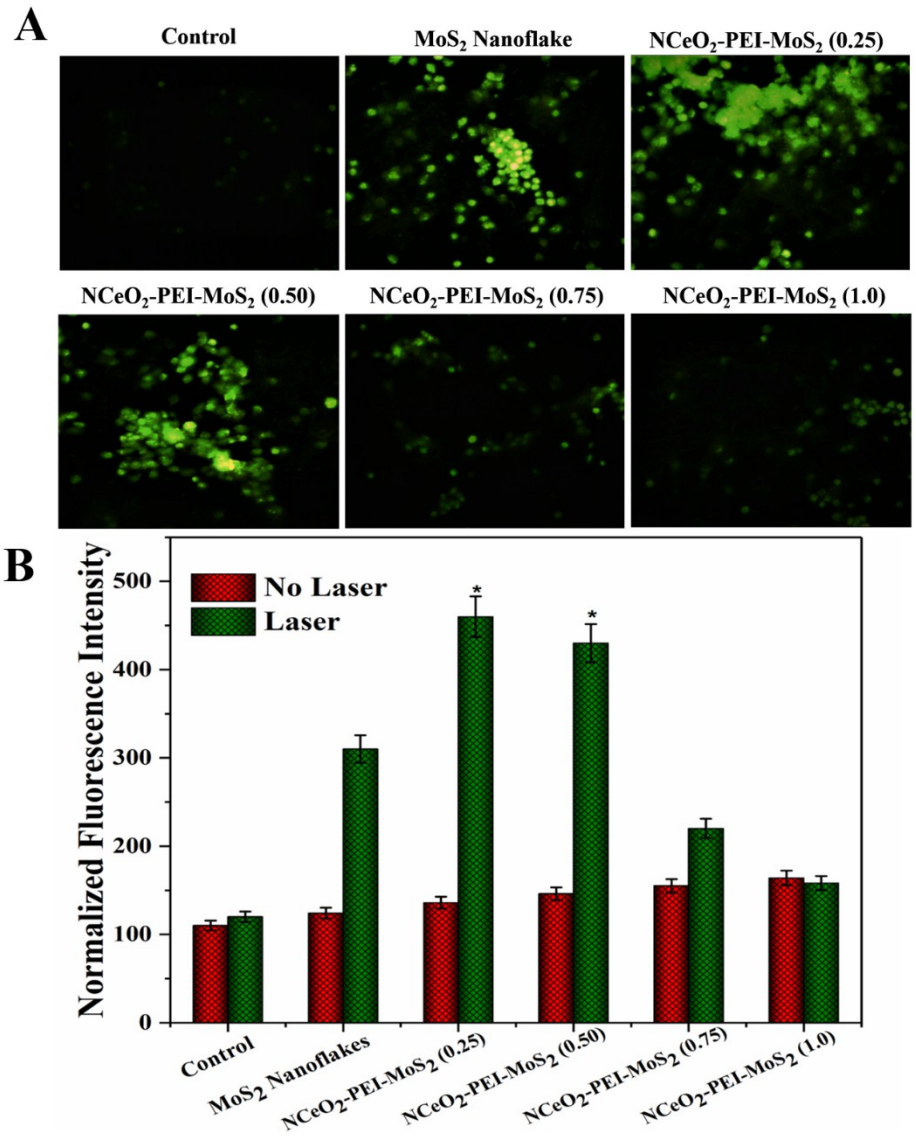

Figure S12. ROS production in DCFH-DA stained MDA-MB-231 cells without and with laser treatment at 808 nm for 5 min (20x magnification).

After irradiation at 808 nm for 5 min, the intracellular ROS generation of bare MoS_2 and $NCeO_2$-PEI-MoS_2 nanoflakes containing different concentration of $NCeO_2$ were examined in MDA-MB-231 cells by DCFH-DA staining technique. The lower fluorescent intensity was noticed from the control cells with laser irradiation, indicating the low intracellular ROS level in the cells. The rate of ROS generation was moderate in irradiated MDA-MB-231 cells with bare MoS_2 nanoflakes, suggesting moderate level of ROS generation and cytotoxicity. When the fluorescent intensity was measured in the suspension containing flakes modified with $NCeO_2$ concentration of 0.25 and 0.5 mg/mL, the intensity of green fluorescence was higher in MDA-MB-231 cells. It is worth noting that nanoflakes prepared with $NCeO_2$ concentration of > 0.5 mg/mL indicated minimal fluorescence intensity. It indicated that the fluorescence intensity increased

as a function $NCeO_2$ concentration up to 0.5 mg/mL and started to decrease at concentration of > 0.5 mg/mL. The lower fluorescent intensity at higher concentration demonstrated that the temperature increase caused by flakes prepared with $NCeO_2$ concentration of > 0.5 mg/mL is not enough to improve ROS generation. These findings revealed that $NCeO_2$ concentration onto MoS_2 nanoflakes significantly influences ROS generation during the PTT therapy.

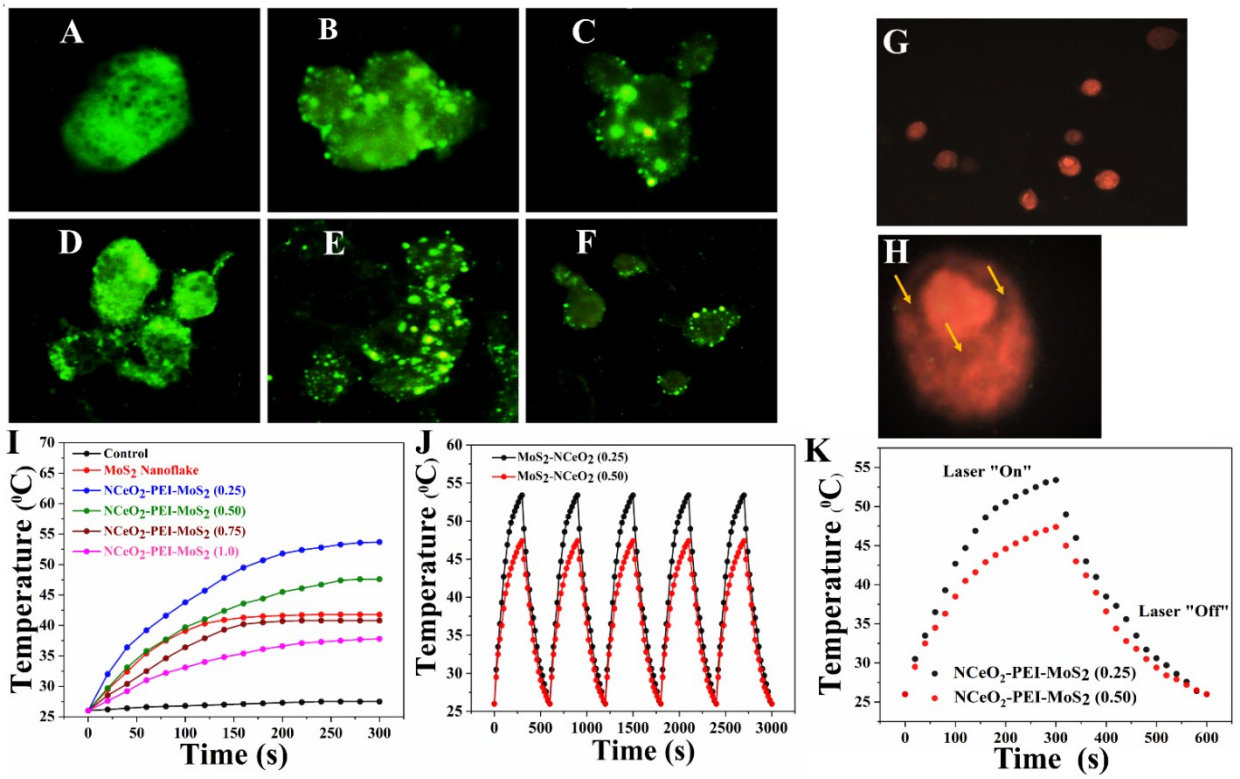

Figure S13. Fluorescence microscopic images reveal ROS mediated apoptosis in DCFH-DA stained MDA-MB-231 cells after treated with $NCeO_2$- PEI-MoS_2 nanoflakes at different time intervals. (A) Control (B) 3 h (C) 6 h (D) 12 h (E) 18 h (F) 24 h. (G-H) Initiation of apoptosis mechanism. In vitro photothermal-property characterization of $NCeO_2$-PEI-MoS_2 nanoflakes (I-K). (I) The photothermal-heating curves of different formulations of $NCeO_2$-PEI-MoS_2 nanoflakes and (J and K) repeated heating-cooling profiles of $NCeO_2$-PEI-MoS_2 nanoflakes with $NCeO_2$ concentration of 0.25 and 0.50 mg/mL in aqueous solution after 808 nm laser irradiation at 0.5 W/cm^{-2} for five laser on/off cycles.

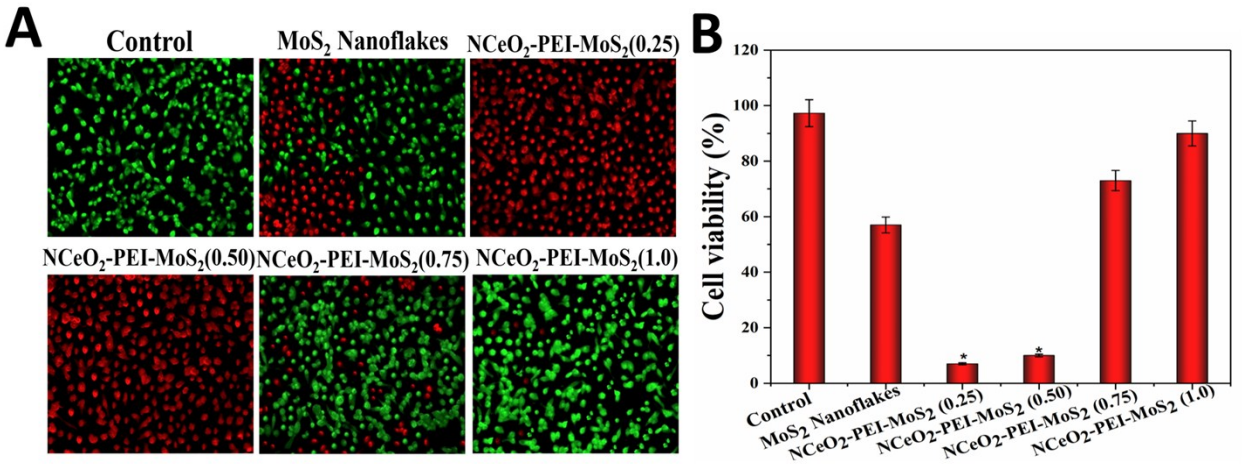

Figure S14. (A) Fluorescense microscopic images of MDA-MB-231 cells after irradiation with 808 nm laser light and (B) their cell viability as a function of $NCeO_2$ concentration.

References

1. T. S. Wu, Y. W. Chen, S. C. Weng, C. N. Lin, C. H. Lai, Y. J. Huang, H. T. Jeng, S. L. Chang & Y. L. Soo, *Sci. Report.*2017, **7**, 4715.
2. M. El Khalifi, F. Picaud and M. Bizi, *Anal. Methods*, 2016,**8**, 5045-5052.
3. Ansari, J.P. Labis, M. Alam, S. M. Ramay, N. Ahmad, A. Mahmood, *Acta Metall. Sin.*, 2016, **29**, 265–273
4. T. Taniguchi, T. Watanabe, N. Sugiyama, A. K. Subramani, H. Wagata, N. Matsushita and M. Yoshimura, *J. Phys. Chem. C*, 2009, **113**, 19789–19793.

Manuscript Images

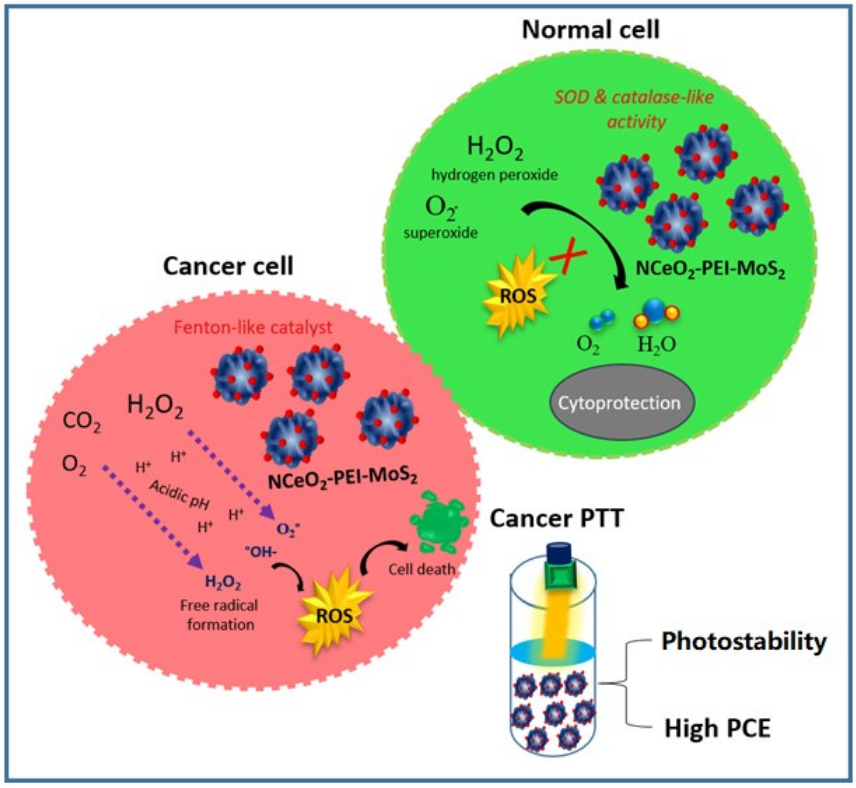

Graphical abstract

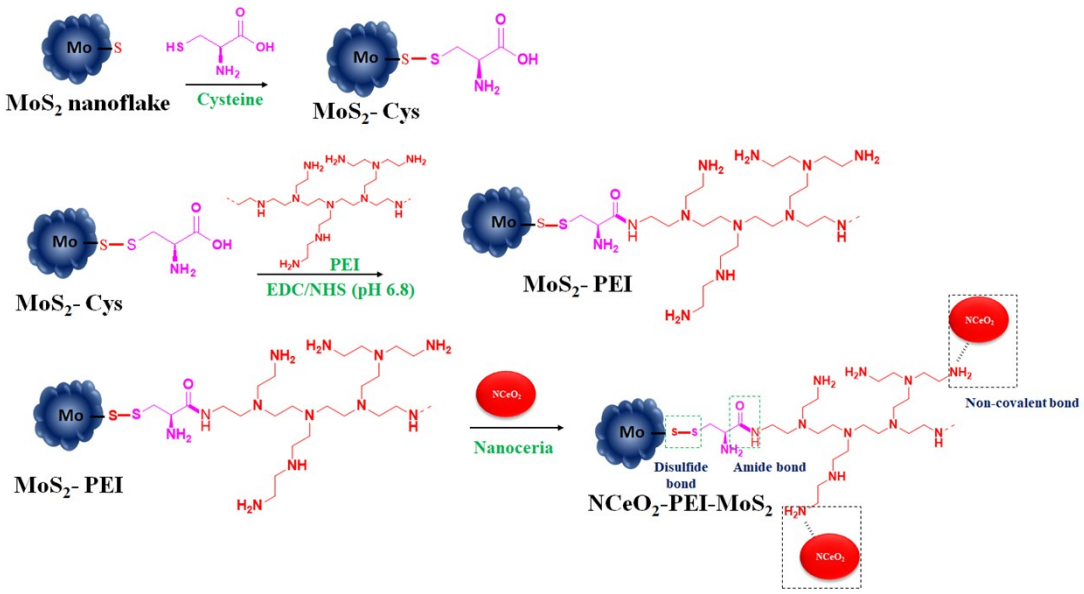

Scheme 1. Schematic representation reveals the fabrication route of $NCeO_2$ decorated PEI coated MoS_2 nanoflake.

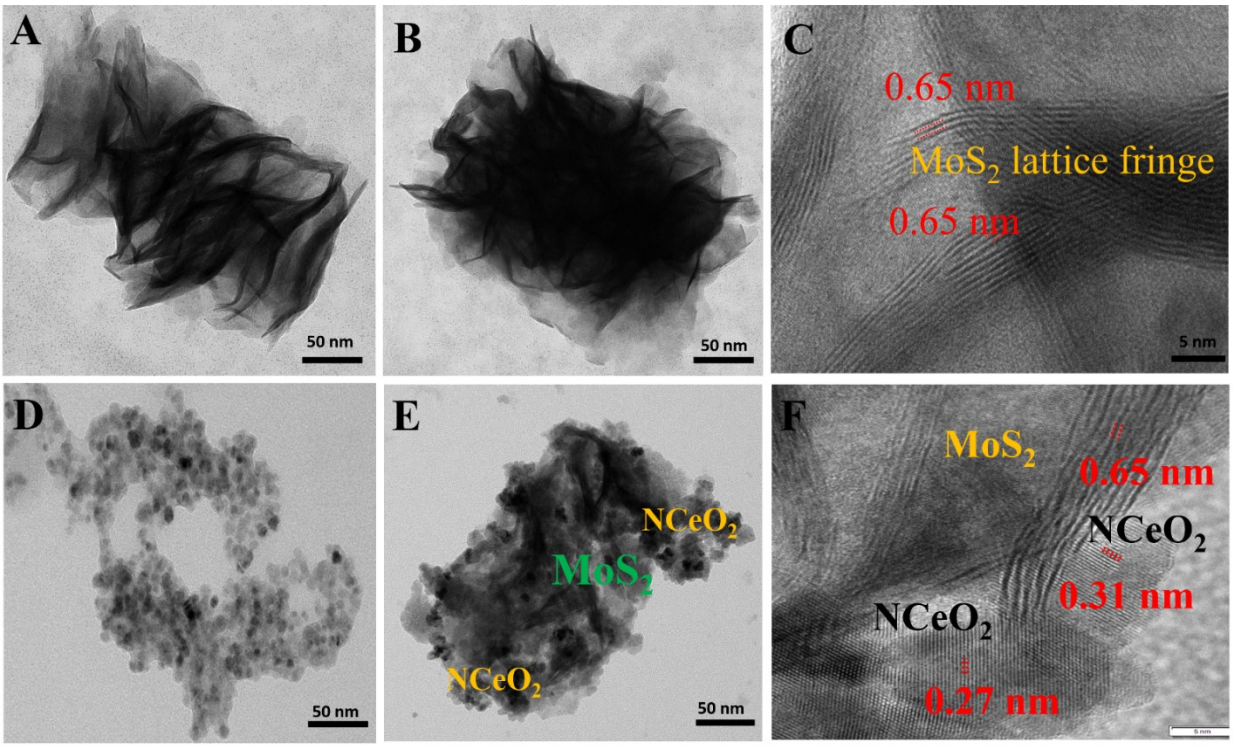

Figure 1. Morphological and structural characterization of (A-C) bare MoS_2 nanoflakes (D) $NCeO_2$ and (E and F) $NCeO_2$ decorated MoS_2 nanoflakes by HR-TEM analysis.

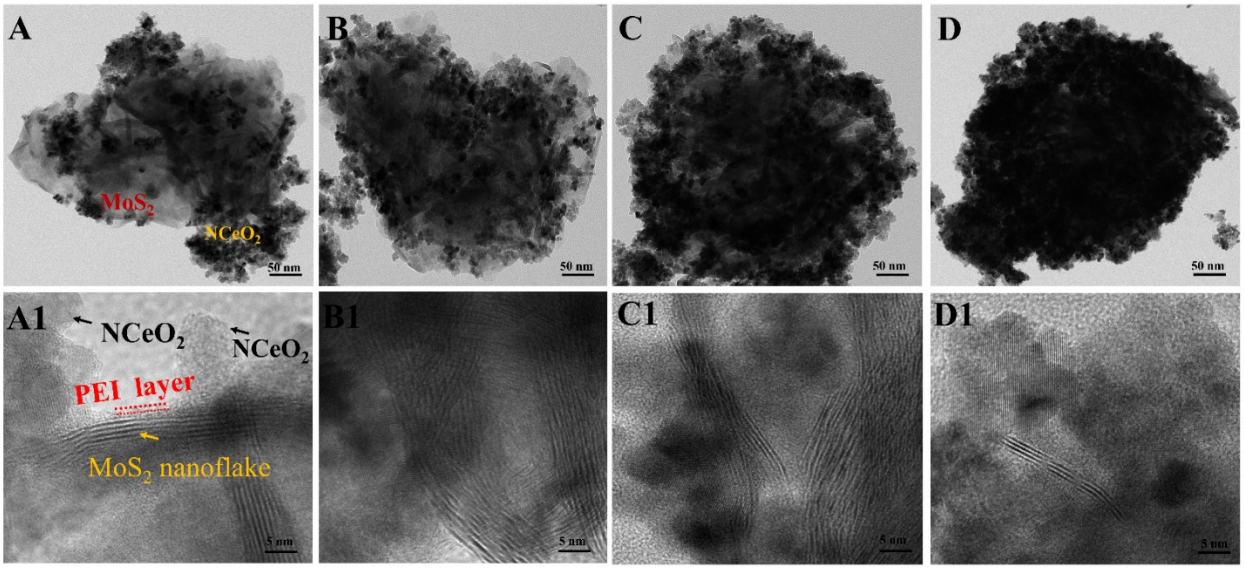

Figure 2. Morphological and structural characterization of $NCeO_2$ decorated MoS_2 nanoflakes as a function of $NCeO_2$ concentration. $NCeO_2$ concentration of (A, A1) 0.25, (B, B1) 0.50, (C, C1) 0.75 and (D, D1) 1 mg/mL were used for decoration onto PEI coated flower-like MoS_2 nanoflakes. Top frame shows the morphology and bottom frame shows lattice fringes of $NCeO_2$ decorated MoS_2 nanoflakes.

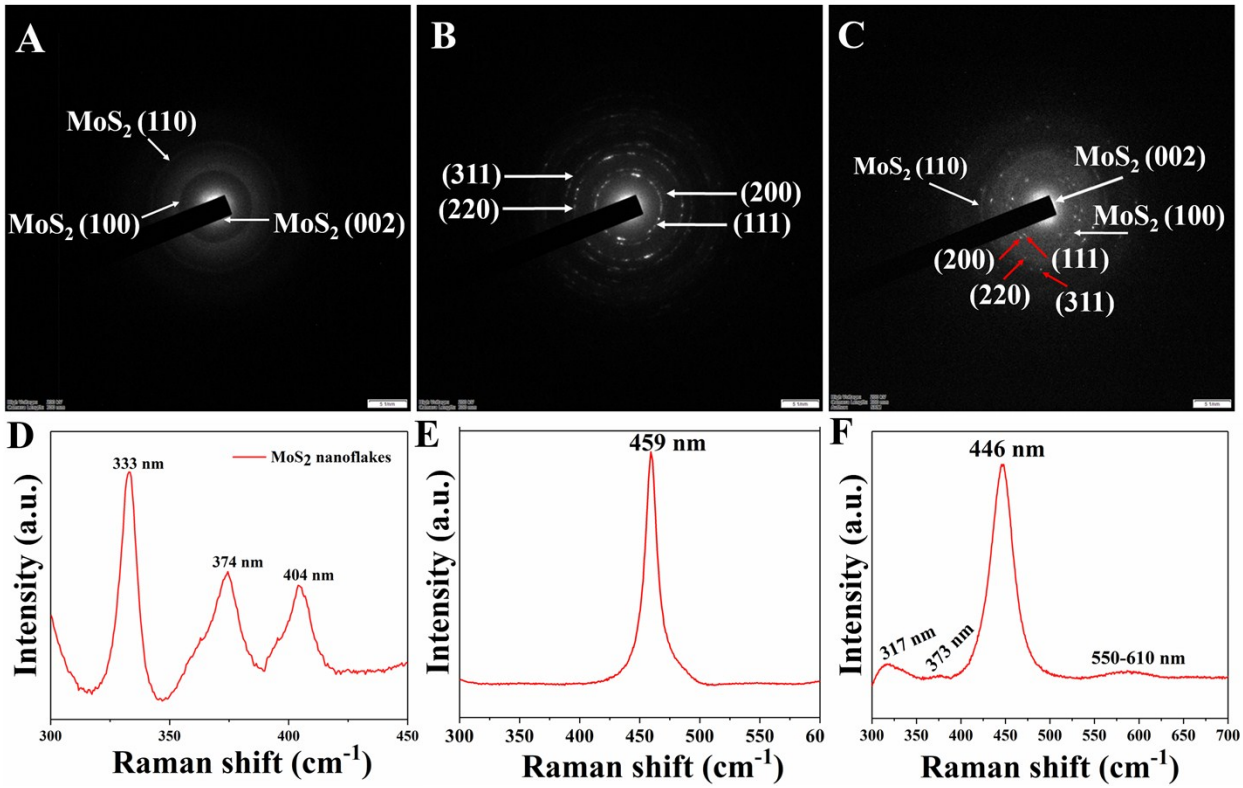

Figure 3. The SAED pattern of (A) bare MoS_2 nanoflakes, (B) $NCeO_2$ and (C) $NCeO_2$-PEI-MoS_2 nanoflakes. Raman spectra of (D) bare MoS_2 nanoflakes, (E) $NCeO_2$ and (F) $NCeO_2$-PEI-MoS_2 nanoflakes.